CONF-970436--1

SAN096-2618C
SAND--96-2618C

The Growth of InAsSb/InAsP Strained-Layer Superlattices for Use in Infrared Emitters*

R. M. Biefeld, A. A. Allerman, S. R. Kurtz,

Sandia National Laboratory, Albuquerque, NM 87185-0601

and J. H. Burkhart

Idaho State University, Pocatello, ID 83201

Abstract

We describe the metal-organic chemical vapor deposition growth of InAsSb/InAsP strained-layer superlattice (SLS) active regions for use in mid-infrared emitters. These SLSs were grown at 500 °C, and 200 torr in a horizontal quartz reactor using TMIn, TESb, AsH_3, and PH_3. By changing the layer thickness and composition we have prepared structures with low temperature (≤20K) photoluminescence wavelengths ranging from 3.2 to 4.4 μm. Excellent performance was observed for an SLS LED and both optically pumped and electrically injected SLS lasers. An optically pumped, double heterostructure laser emitted at 3.86 μm with a maximum operating temperature of 240 K and a characteristic temperature of 33 K.. We have also made electrically injected lasers and LEDs utilizing a GaAsSb/InAs semi-metal injection scheme. The semi-metal injected, broadband LED emitted at 4 μm with 80 μW of power at 300K and 200 mA average current. The InAsSb/InAsP SLS injection laser emitted at 3.6 μm at 120 K.

Introduction

Chemical sensor and infrared countermeasure technologies would become viable with the availability of high power, mid-infrared (3-6 μm) lasers and LEDs operating near room temperature. However, the performance of mid-infrared emitters has been limited by nonradiative recombination processes (usually Auger recombination), which dominate radiative recombination in narrow bandgap semiconductors. Auger recombination can be suppressed in "band-structure engineered", strained InAsSb heterostructures. In order to reduce Auger recombination in mid-infrared (2-6 μm) lasers, several narrow bandgap III-V, strained-layer superlattices (SLSs) have been explored using metal-organic chemical vapor deposition (MOCVD) and molecular beam epitaxy (MBE).[1-11] In both type I and type II SLS laser active regions, holes are confined to compressively strained layers, producing a low in-plane, effective mass ($|3/2,\pm3/2\rangle$) hole ground state. In compressively strained InAsSb SLSs, it is necessary to maximize the light-heavy ($|3/2,\pm1/2\rangle$ - $|3/2,\pm3/2\rangle$) hole splitting to suppress Auger recombination. For example, we have investigated the electronic properties of InGaAs/InAsSb SLSs, and we find that the light-heavy hole splitting (≈ 30 meV) is insufficient to achieve maximum suppression of Auger recombination.[1,12,13] InAsSb SLSs incorporating barrier layers with larger valence band offsets are required to maximize the light-heavy hole splitting through quantum confinement. Towards this goal, MBE-grown InAsSb/InAlAs and InAsSb/InAlAsSb SLS lasers have been examined with encouraging results.[2,8] In this work, we report the properties of the first InAsSb/InAsP SLS materials and devices. The InAsSb/InAsP SLS is an "MOCVD variant" of the most promising type I, strained InAsSb heterostructures for Auger suppression, and a miscibility gap, reported for InAlAsSb quaternaries,[8] has not been encountered for InAsP. Incorporating InAsP as a barrier layer in the active region will introduce a larger valence band offset than either of the offsets between InAs or InGaAs and InAsSb. Compared with other compressively strained InAsSb devices, initial

tests on InAsSb/InAsP SLS lasers and LEDs show state-of-the-art performance. We report on the synthesis of these materials by MOCVD and their use in improved 3-6 μm, mid-infrared optoelectronic heterojunction emitters.

Experimental

This work was carried out in a previously described MOCVD system[14,15]. We used ethyldimethylamine alane (EDMAA), triethylantimony (TESb) and 100% arsine (AsH_3) as the sources for Al, Sb and As respectively, for the growth of $AlAs_xSb_{1-x}$ cladding layers. Triethylgallium (TEGa), arsine and TESb were used to grow a 400 to 2500Å GaAsSb cap on all samples to keep the $AlAs_xSb_{1-x}$ layer from oxidizing and to serve as a semi-metal electron injector.[10] Hydrogen was used as the carrier gas at a total flow of 8 slpm.

The InAsSb/InAsP SLSs were also grown by MOCVD on n-type InAs substrates. The InAsSb/InAsP SLSs were grown at 500 °C, and 200 torr in a horizontal quartz reactor using trimethylindium (TMIn), TESb, 10 % AsH_3 in hydrogen, 100 % PH_3 and hydrogen as the carrier gas. The InAsSb layers were grown using a V/III ratio of 15 to 21 and an $AsH_3/(AsH_3+TESb)$ ratio of 0.59 to 0.71 at a growth rate of 2.5 Å/second. A 15 second purge, with reactants switched out of the chamber, was used between each layer. The InAsP layers were grown using a V/III ratio of 217 and an AsH3/(AsH3+ PH3) ratio of 0.02 with an identical growth rate of 2.5 Å/second. The SLSs were lattice matched to InAs with $\Delta a/a < 0.0004$. The SLS composition and strain were determined by double crystal x-ray diffraction.

Infrared photoluminescence (PL) was measured on all samples at 14 K up to 300 K using a double-modulation, Fourier-transform infrared (FTIR) technique which provides high sensitivity, reduces sample heating, and eliminates the blackbody

background from infrared emission spectra. Injection devices (both LEDs and lasers) also were characterized with double modulation FTIR.

Results And Discussion

Growth and Characterization of InAsP/InAsSb SLSs

The growth rate of the InAsSb/InAsP SLSs was found to be proportional to the TMIn flow into the reaction chamber and independent of the TESb, PH_3, and AsH_3 flow. The crystal quality of the SLSs was excellent with 3 to 4 orders of x-ray diffraction satellite peaks typically observed (See Figure 1(a)). The variation of the Sb composition for the InAsSb layer as a function of $AsH_3/(AsH_3+TESb)$ ratio in the vapor is shown in Figure 2. The Sb composition could be varied between 0.13 to 0.2 while maintaining constant layer thickness for both the InAsSb and InAsP layers.

The electrically injected laser structure consisted of 2.5 μm of undoped AlAsSb top and bottom claddings, a p-GaAsSb / n-InAs semi-metal electron injector, and a 10 to 40 period InAsSb/InAsP SLS active region. The satellite peaks observed in the bottom cladding layer growth (Figure 1(b)) are from an InAsSb/InAsP SLS used as a buffer on the InAs substrate to improve surface morphology of the 2.5 μm AlAsSb cladding layer for the lasers. The same SLS structure used in the active region was used for the buffer. The x-ray diffraction pattern for a complete electrically injected laser structure with 2.5 μm of AlAsSb in both the top and bottom cladding layers is shown in Figure 1(c).

The PL peak wavelength dependence on composition for the SLSs is shown in Figure 3. For a change of composition from x = 0.13 to 0.20 the PL peak changes from 3.5 to 4.4 μm. Room temperature photoluminescence was observed out to 5.0 μm. The variation of PL wavelength versus thickness of the InAsSb well is shown in Figure 4. The wavelength could be varied from 3.2 to 3.8 μm for a change in thickness from 45 to 108 Å. For layers thicker than approximately 90 Å the x-ray diffraction patterns broadened, indicating the presence of dislocations.

The band alignments and quantum confinement states for a representative *InAsSb/InAsP SLS* active region are shown in Figure 5. The energy levels for this $InAs_{0.88}Sb_{0.12}$ / $InAs_{0.76}P_{0.24}$ (80 Å / 80 Å) SLS were determined using a transfer matrix, 8x8 k•p calculation. Based on previous measurements of our ordered and phase separated, MOCVD-grown, InAsSb alloys, the estimated bandgap of the unstrained $InAs_{0.88}Sb_{0.12}$ alloy was 259 meV.[12,16] SLS valence band offsets vary linearly with composition from unstrained InAs/InSb and InAs/InP valence band offset values, 0.39 eV[12,16] and -0.56 eV[13] respectively. When used as the active region, the SLS in Figure 5 will emit at 349 meV (3.6 μm) at low temperature. We estimate that the SLS has a light-heavy hole splitting of 69 meV, and emitters incorporating these SLSs should display improved performance over earlier devices with MOCVD-grown active regions. Limited by critical layer thickness, longer wavelength InAsSb/InAsP SLSs with higher Sb and P content will display even larger light-heavy hole splittings.

InAsSb/InAsP SLS Active Region Optically Pumped and Injection Lasers and LEDs

An LED was constructed with a 0.7 μm thick, n-type, $InAs_{0.88}Sb_{0.12}$ /$InAs_{0.75}P_{0.25}$ (80 Å / 82 Å) SLS active region. As for the previously published MQW structures,[10] a semi-metal layer consisting of a 500 Å thick GaAsSb (p-type) and a 500 Å thick InAs (n-type) heterojunction provided electrical injection for the LED. A 1 mm^2 piece of the wafer was mounted onto a header with a parabolic collector. The top contact of the LED was a 0.02" diameter Ti/Au dot. A 300K emission spectrum for the LED is shown in Figure 6(a). The large emission peak at 4 μm originates from the SLS active region; electron-hole recombination in the InAs layer produces the small peak at 360 meV. The InAsSb/InAsP SLS LED is the brightest 4 μm, room temperature device that we have produced with MOCVD. Operating the device at 1 kHz, 50% duty cycle, 200 mA average current, the average output power of the LED was 80 μW at 300 K. At 80 K the output

power of the LED was 24x that observed at 300 K. The output power of our SLS device (300 K) was 5-6x that measured with the same current for LPE-grown, InAsSb alloy LEDs, obtained commercially.[17]

To avoid loss mechanisms associated with electrical injection and to observe lasing with minimum heating, InAsSb/InAsP SLS lasers were characterized using low duty-cycle optical pumping. An optically pumped laser was grown on an InAs substrate with a 2.5 μm thick $AlAs_{0.16}Sb_{0.84}$ lower cladding. On top of the cladding, the active region was a 1.0 μm thick, $InAs_{0.89}Sb_{0.11}/InAs_{0.77}P_{0.23}$ (83 Å / 87 Å) SLS. For the limited number of devices studied, neither a top cladding nor a semi-metal injection layer seemed to significantly affect laser performance under optical pumping. The SLS laser was pumped with a Q-switched Nd:YAG (1.06 μm, 20 Hz, 10 nsec pulse, focused to a 200 μm wide line), and emission was detected with an FTIR spectrometer operated in a step-scan mode. Due to the low rep-rate of the pump, approximately a 4 hour scan was required to obtain an interferogram with resolution ≥ 2 cm^{-1}.

Laser emission was observed from cleaved bars, 1000 μm wide, with uncoated facets. A lasing threshold and spectrally narrowed, laser emission was seen from 80 K through 240 K, the maximum temperature where lasing occurred. (See Figure 6(b) and 7(a)) As shown in Figure 6(b), the PL linewidth is ≈ 25 meV at 80K, but above threshold, the laser emission, narrowed to 3-5 meV depending on the sample, is superimposed on the broad spontaneous emission. The laser emission linewidth is limited by inhomogenieties in the material and the presence of multiple, unresolved longitudinal modes; similar behavior was observed in optically pumped type II, GaInSb/InAs lasers.[7,9] The wavelength of our laser shifts from 3.57 μm to 3.85 μm due to the decrease in bandgap over the 80-240K temperature range. At 80 K, peak powers >100 mW could be obtained. In Figure 6(b), laser emission was 6 meV higher in energy than the PL peak; for other InAsSb/InAsP SLS lasers tested, laser emission was at the PL peak energy. Generally, InAsSb/InAsP SLS laser emission occurred nearer to the peak of the PL emission than previously reported for

MOCVD-grown devices with pseudomorphic InAsSb multiple quantum well active regions[1,5,10,12]. The temperature dependence of the SLS laser threshold is described by a characteristic temperature, $T_0 = 33$ K, over the entire range. (See Figure 7(b))

In several areas, the InAsSb/InAsP SLS laser approached performance records for III-V, bipolar lasers of comparable wavelength. We report the lowest threshold power, highest characteristic temperature, and highest operating temperature for InAsSb lasers at ≈ 3.9 μm, obtained either with pulsed injection[2,10,18] or pulsed optical pumping.[19,20] Recently, Malin et al. reported record-setting performance for a type II, 4 μm GaInSb/InAs SLS laser pumped with a pulsed Ho:YAG laser (2.06 μm, 10 Hz).[9] The characteristic temperature of our InAsSb/InAsP SLS device is comparable to that reported for the type II device (T_o= 35 K).[9] The maximum operating temperature (270K) and threshold power (P_{th}= 100 kW/ cm^2 @ 240K) of the type II device are marginally improved over our laser,[9] and unpublished results for the optically pumped, type II lasers report even further improvement.[19] However, excitation with the Ho:YAG will produce less heating and may explain much of the improvement.[20] InAsSb/InAsP, InAsSb/InAlAs, or GaInSb/InAs SLS active regions should suppress Auger recombination, and initial results for these lasers have been promising. However, ≈ 4 μm lasers with these active regions have not yet demonstrated characteristic temperatures larger than ≈ 40 K.[2,9,10,19]

We have recently demonstrated InAsSb/InAsP SLS injection lasers at 3.6 μm and 120 K. We speculate that injection and transport of carriers in the SLS is presently limiting the performance of these devices.

Conclusions

We have evaluated InAsSb/InAsP SLSs as active regions for MOCVD-grown, mid-infrared lasers and LEDs. Band structure calculations for these SLSs indicate that large light-heavy hole splittings (≥ 70 meV) can be achieved to suppress Auger recombination.

X-ray and optical characterization of the SLSs indicate very high crystalline quality for the MOCVD-grown material and electronic properties consistent with our model of the SLS. Excellent performance was observed for an SLS LED and an optically pumped SLS laser. The semi-metal injected, broadband LED emitted at 4 μm with 80 μW of power at 300K, 200 mA average current. The optically pumped laser displayed 3.86 μm emission at 240 K, the maximum operating temperature of the laser, and a characteristic temperature of 33 K. InAsSb/InAsP SLS laser operating temperature, characteristic temperature, and threshold power values are state-of-the-art for InAsSb lasers at ≈ 4 μm. Also, injection InAsSb/InAsP lasers were demonstrated. With nominal improvements in materials and processing and the further development of multi-stage active regions, MOCVD-grown InAsSb devices should be able to satisfy the system requirements for use in chemical sensor and infrared countermeasure technologies in the near future.

Acknowledgments

We thank J. A.Bur for technical support. Our work was supported by the U.S. Dept. of Energy under contract No. DE-AC04-94AL85000. Sandia is a multiprogram laboratory operated by Sandia Corporation, a Lockheed Martin Company, for the United States Department of Energy.

References

1. S. R. Kurtz, R. M. Biefeld, A. A. Allerman, A. J. Howard, M. H. Crawford, and M. W. Pelczynski, Appl. Phys. Lett. **68**, 1332 (1996).
2. H. K. Choi and G. W. Turner, Appl. Phys. Lett. **67**, 332 (1995).
3. Y-H. Zhang, Appl. Phys. Lett. **66**, 118 (1995).
4. R. M. Biefeld, A. A. Allerman, and M. W. Pelczynski, Appl. Phys. Lett. **68**, 932 (1996).
5. S. R. Kurtz, R. M. Biefeld, L. R. Dawson, K. C. Baucom, and A. J. Howard, Appl. Phys. Lett. 64, 812 (1994).
6. D. Z. Garbuzov, R.U Martinelli, R.J. Menna, P.K. York. H. Lee, S. Y. Narayan, and J. C. Connolly, Appl. Phys. Lett. 67, 1346 (1995).
7. D.H. Chow, R.H. Miles, T.C. Hasenberg, A.R. Kost, Y.-H. Zhang, H.L. Dunlap and L. West, Appl. Phys. Lett. 67, 3700 (1995).
8. H. K. Choi, G. W. Turner, M. J. Manfra, and M. K. Connors, Appl. Phys. Lett. 68, 2936 (1996).
9. J. I. Malin, J. R. Meyer, C. L. Felix, J. R. Lindle, L. Goldberg, C. A. Hoffman, F. J. Bartoli, C. H. Lin, P. C. Chang, S. J. Murry, R. Q. Yang, and S. S. Pei, Appl Phys. Lett. 68, 2976 (1996).
10. A. A. Allerman, R. M. Biefeld, and S. R.Kurtz, Appl. Phys. Lett. **69**, 465 (1996).
11. R. J. Menna, D. Garbuznov, R. U. Martinelli, and G. H. Olsen (to be published).
12. S. R. Kurtz, R. M. Biefeld, and A. J. Howard, Appl. Phys. Lett. 67, 3331(1995).
13. H. P. Hjalmarson and S. R. Kurtz, Appl. Phys. Lett. **69**, 949 (1996).
14. R. M. Biefeld, K. C. Baucom, and S. R. Kurtz, J. Crystal Growth, **137**, 231 (1994).
15. R. M. Biefeld, J. Crystal Growth, **75**, 255 (1986).
16. S. R. Kurtz and R. M. Biefeld, Appl. Phys. Lett. **66**, 3331 (1995).

17. Our device was compared with a 4.2 μm LED obtained from RMC Ltd., Moscow, Russia.

18. H. K. Choi, G. W. Turner, and H. Q. Le, Inst. Phys. Conf. Ser. 144, 209 (1995).

19. C. L. Felix, J. R. Meyer, I Vurgaftman, C. H. Lin, S. J. Murry, D. Zhang, and S. S. Pei, Photon. Tech. Lett. (accepted for publication).

20 . H. Q. Le, G. W.Turner, J. R. Ochoa, and A. Sanchez, Elect. Lett. 30, 1944 (1994)

Figure Captions

Figure 1. X-Ray diffraction spectra of (a) a 20 period 75Å $InSb_xAs_{1-x}$ / 84Å $InAs_{.76}P_{.24}$ SLS's grown on InAs, (b) a lower $AlAs_{0.16}Sb_{0.84}$ cladding layer (2.5 μm) and a semi-metal $GaAs_{0.92}Sb_{0.08}$ injector grown on top of a 30 period 75Å $InSb_xAs_{1-x}$ / 84Å $InAs_{.76}P_{.24}$ SLS buffer layer grown on InAs, and (c) an injection laser using the same active region as (a) with 40 periods and the lower cladding region of (b) and 2.5 μm of $AlAs_{0.16}Sb_{0.84}$ upper cladding.

Figure 2. Incorporation of Sb into the InAsSb layer as a function of AsH3/(AsH3+ TESb)ratio in the vapor phase for the InAsSb/InAsP SLSs.

Figure 3. Low temperature PL (< 20K) from a 40 period 75Å $InSb_xAs_{1-x}$ / 84Å $InAs_{.76}P_{.24}$ SLS's grown on InAs for different Sb contents in the InAsSb layer.

Figure 4. Low temperature PL (< 20K) from 20 period $InAs_{0.86}Sb_{0.14}$ / 84Å $InAs_{.76}P_{.24}$ SLS's grown on InAs for different InAsSb layer thicknesses.

Figure 5. Band alignments and quantum confinement state energies (drawn to scale) for an $InAs_{0.88}Sb_{0.12}$ / $InAs_{0.76}P_{0.24}$ (80 Å / 80 Å) SLS.

Figure 6. (a) Emission spectrum for an LED with an $InAs_{0.88}Sb_{0.12}$/$InAs_{0.75}P_{0.25}$ (80 Å / 82 Å) SLS active region. The spectrum is distorted by CO_2 absorption lines at 290 meV. (b) Lasing and PL spectra for a laser with an $InAs_{0.89}Sb_{0.11}$ /$InAs_{0.77}P_{0.23}$ (83 Å / 87 Å) SLS active region.

Figure 7. (a) Pulsed laser emission intensity versus optical pump power for various temperatures for an $InAs_{0.89}Sb_{0.11}/InAs_{0.77}P_{0.23}$ (83 Å / 87 Å) SLS active region. (b) Threshold optical pump power versus temperature.

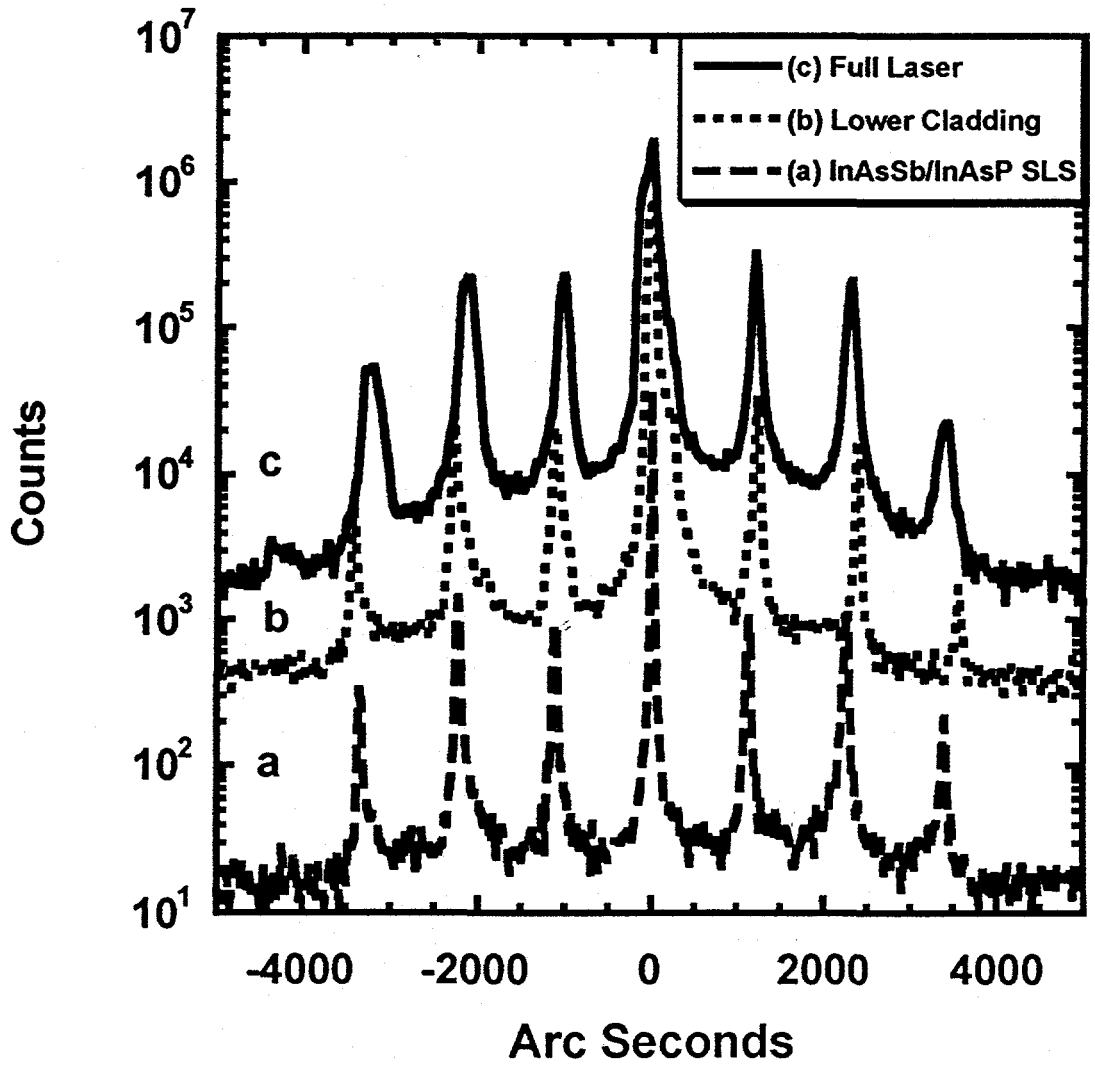
(c) Full Laser
(b) Lower Cladding
(a) InAsSb/InAsP SLS
Counts
10^7
10^6
10^5
10^4
10^3
10^2
10^1
c
b
a
-4000
-2000
0
2000
4000
Arc Seconds

Figure 1.

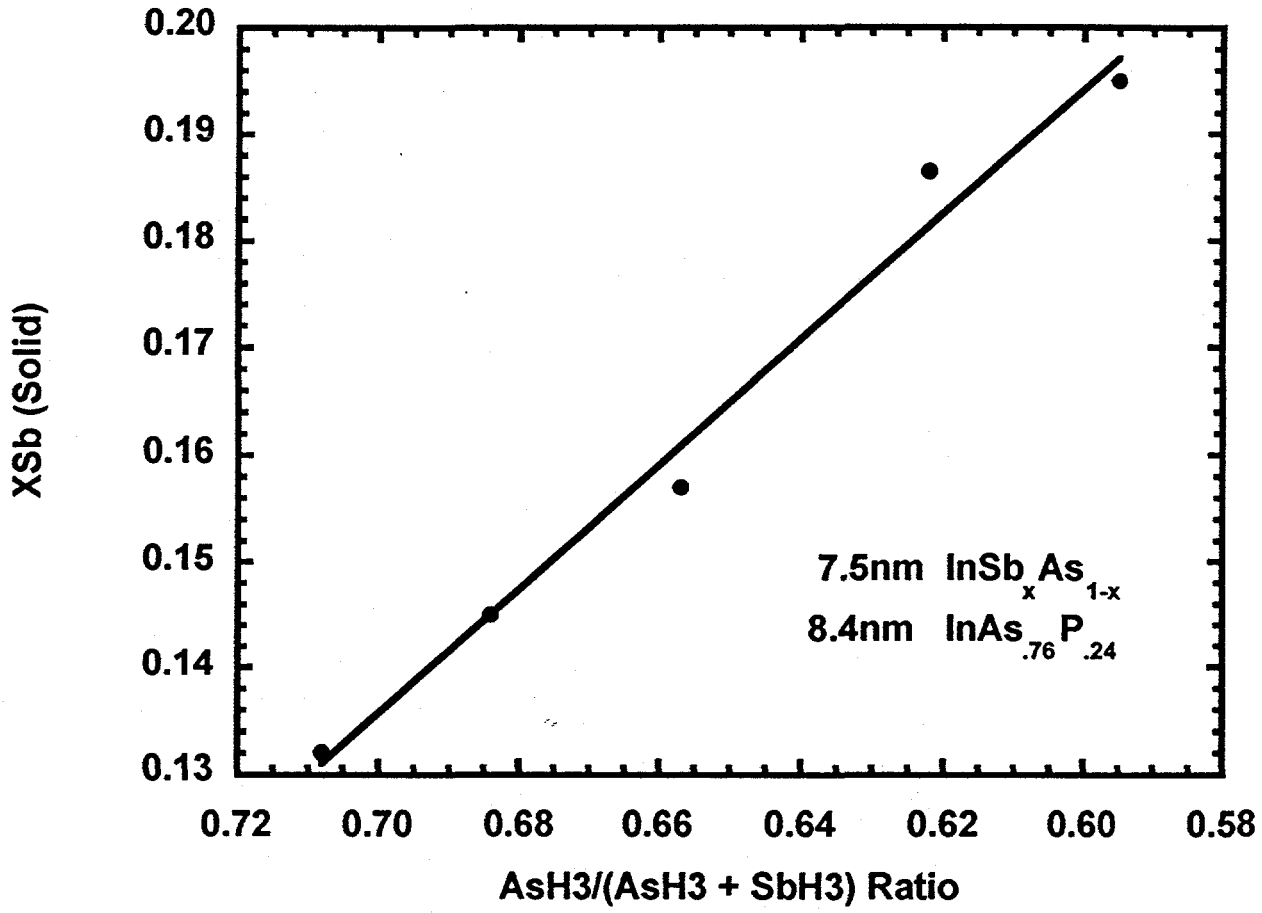
0.20
0.19
0.18
0.17
0.16
0.15
0.14
0.13
XSb (Solid)
0.72
0.70
0.68
0.66
0.64
0.62
0.60
0.58
AsH3/(AsH3 + SbH3) Ratio
7.5nm InSb$_x$As$_{1-x}$
8.4nm InAs$_{.76}$P$_{.24}$

Figure 2.

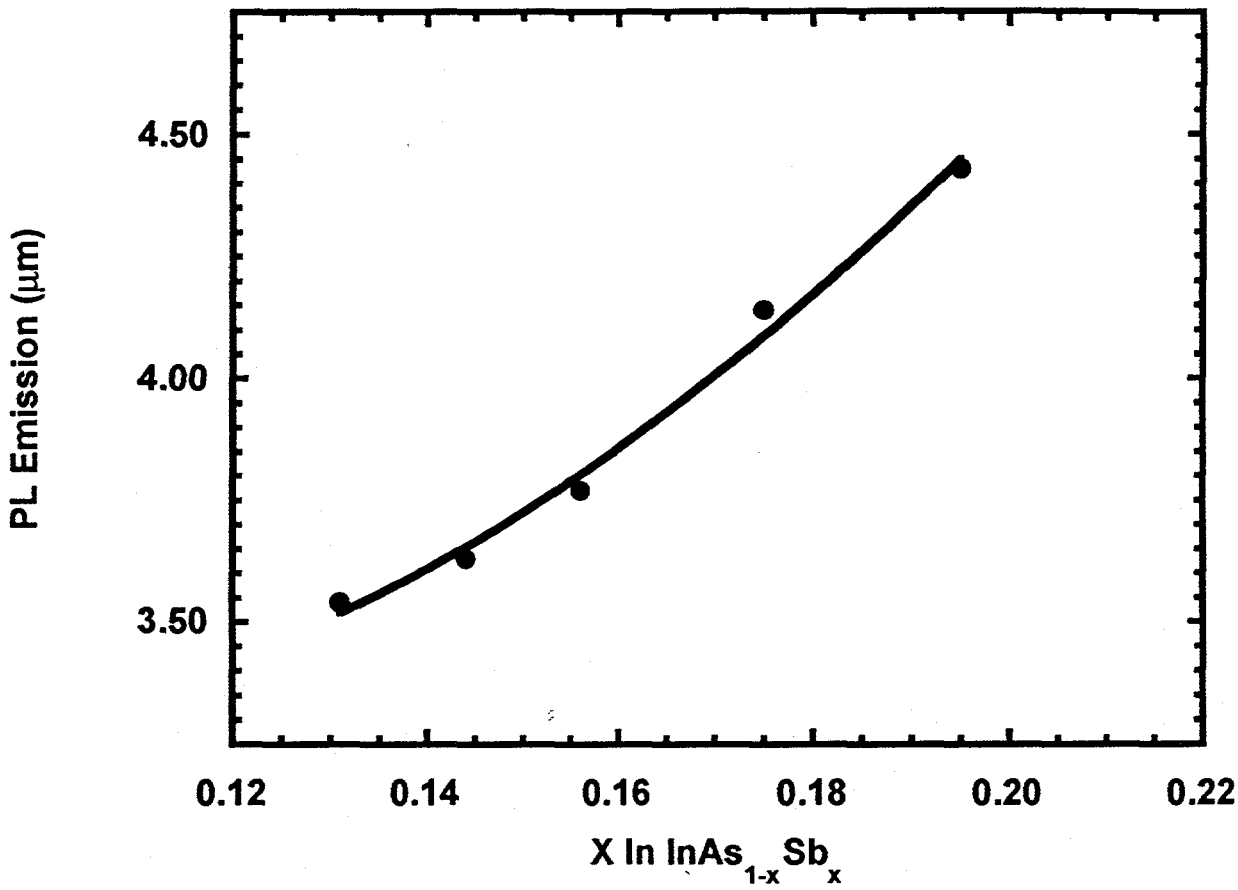
4.50
4.00
3.50
PL Emission (μm)
0.12
0.14
0.16
0.18
0.20
0.22
X In InAs1-xSbx

Figure 3.

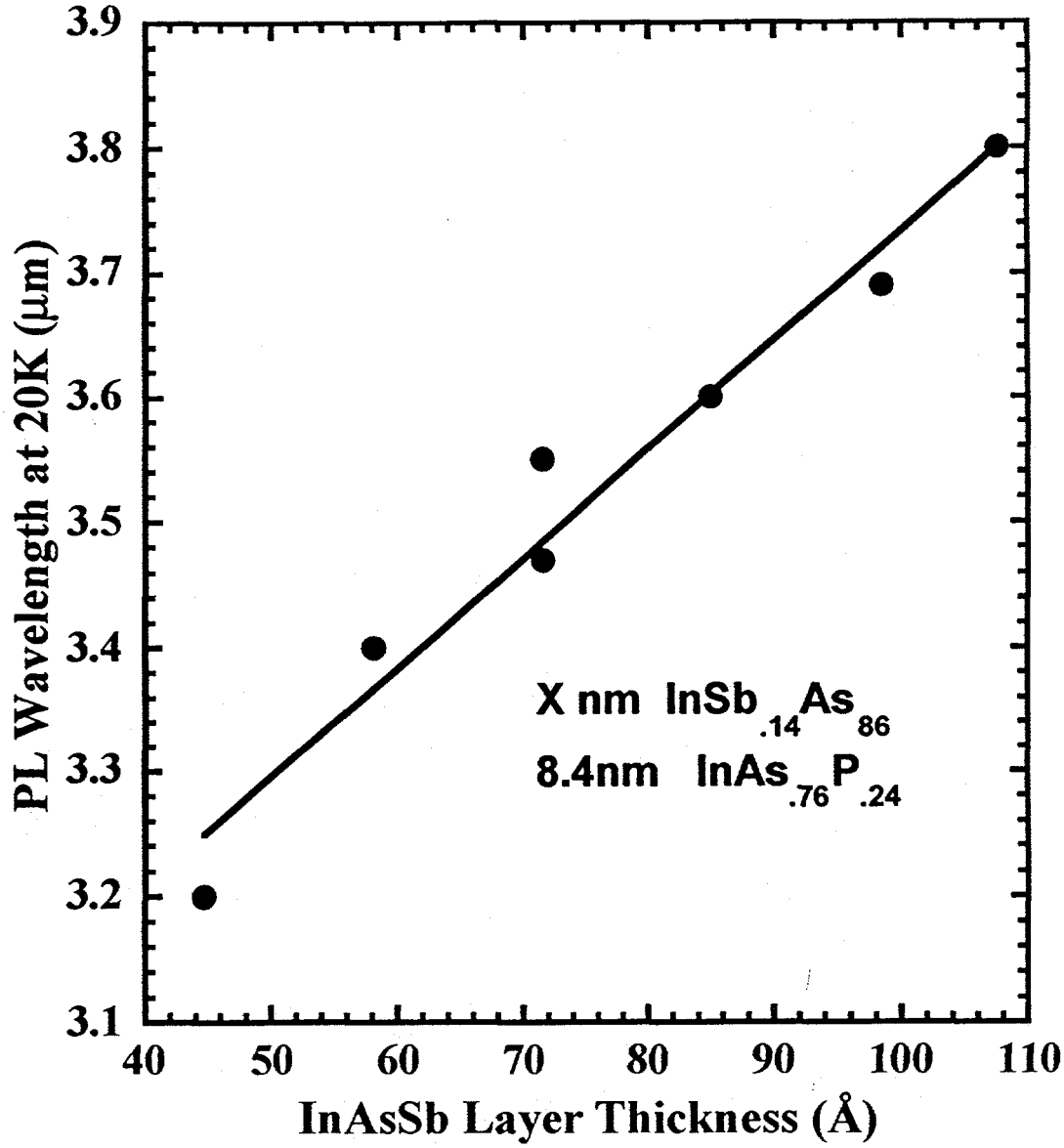
3.9
3.8
3.7
3.6
3.5
3.4
3.3
3.2
3.1
PL Wavelength at 20K (μm)
40
50
60
70
80
90
100
110
InAsSb Layer Thickness (Å)
X nm InSb.14As.86
8.4nm InAs.76P.24

Figure 4.

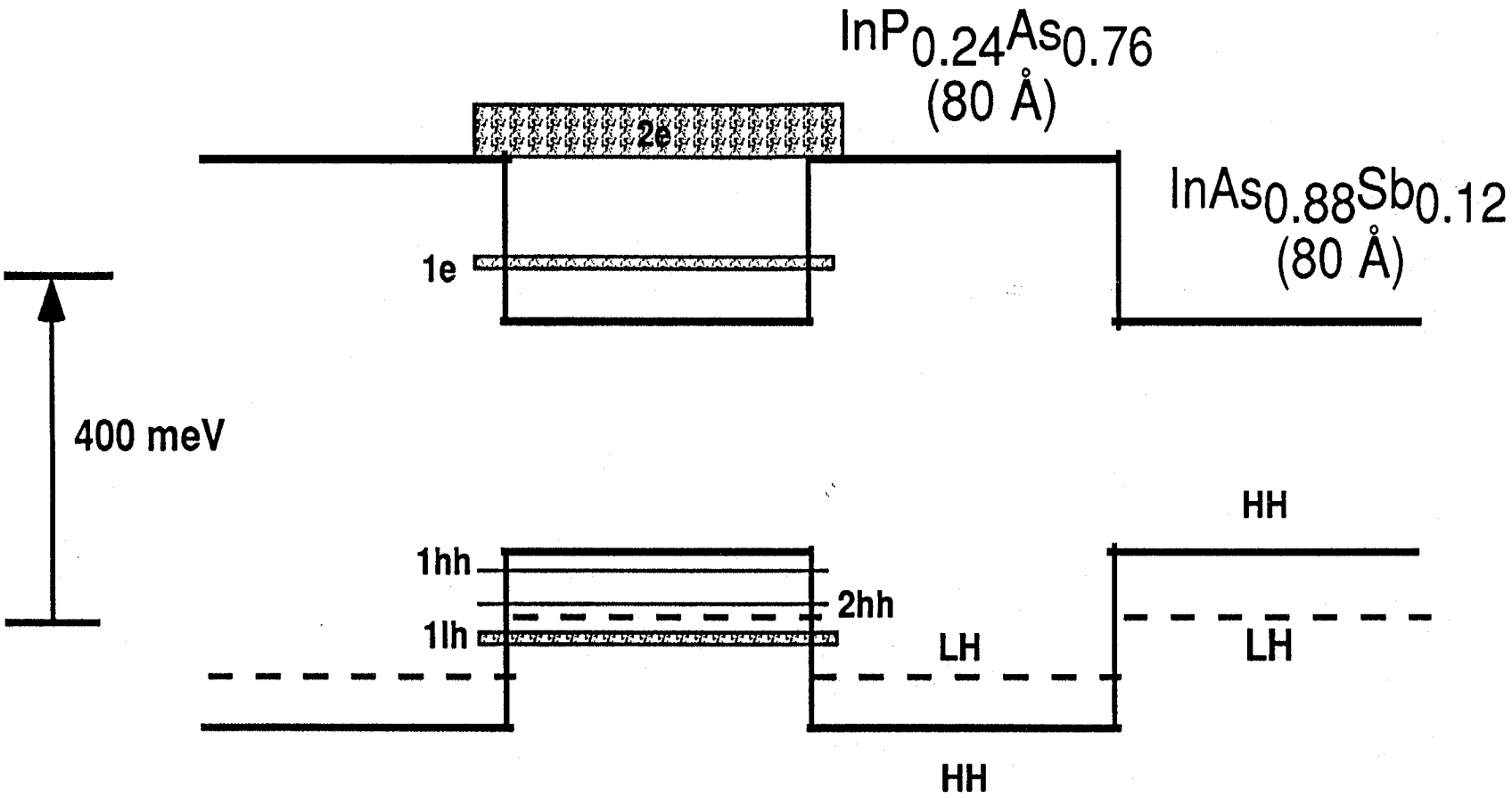
InP0.24As0.76
(80 Å)
2e
InAs0.88Sb0.12
(80 Å)
1e
400 meV
HH
1hh
2hh
1lh
LH
LH
HH

Figure 5.

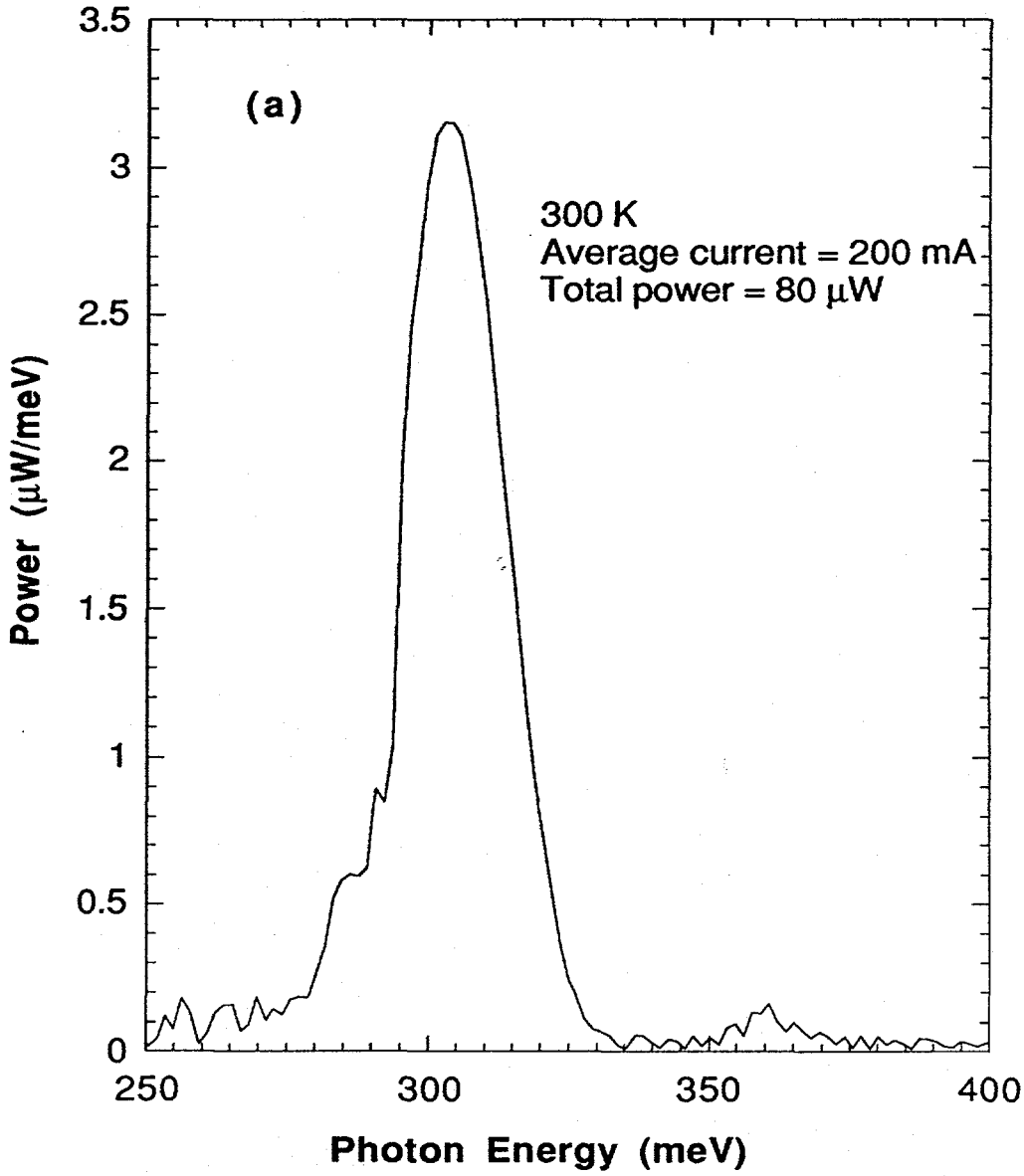
(a)
300 K
Average current = 200 mA
Total power = 80 μW
Power (μW/meV)
Photon Energy (meV)
3.5
3
2.5
2
1.5
1
0.5
0
250
300
350
400

Figure 6(a)

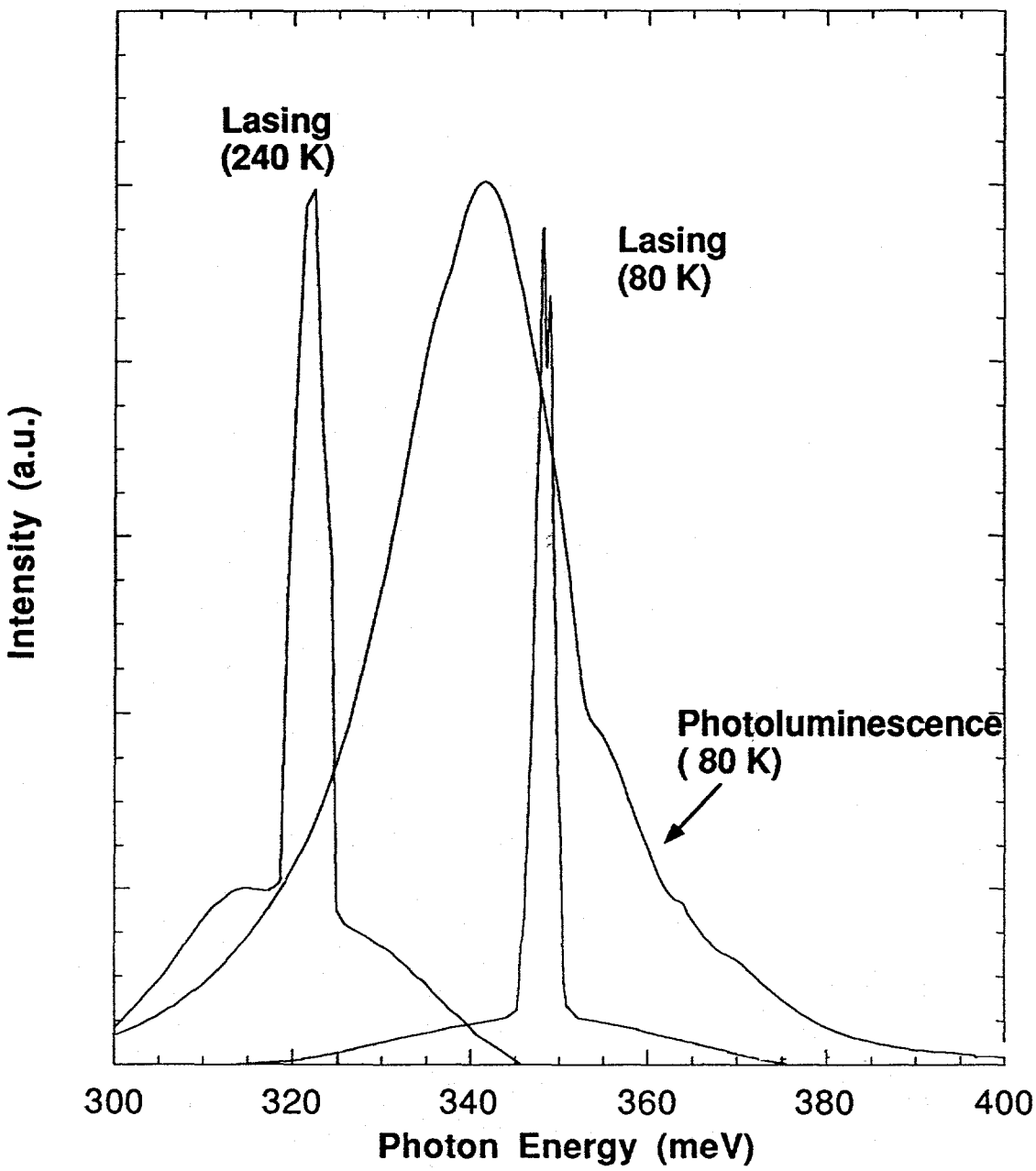
Lasing
(240 K)
Lasing
(80 K)
Photoluminescence
(80 K)
Intensity (a.u.)
300
320
340
360
380
400
Photon Energy (meV)

Figure 6 (b)

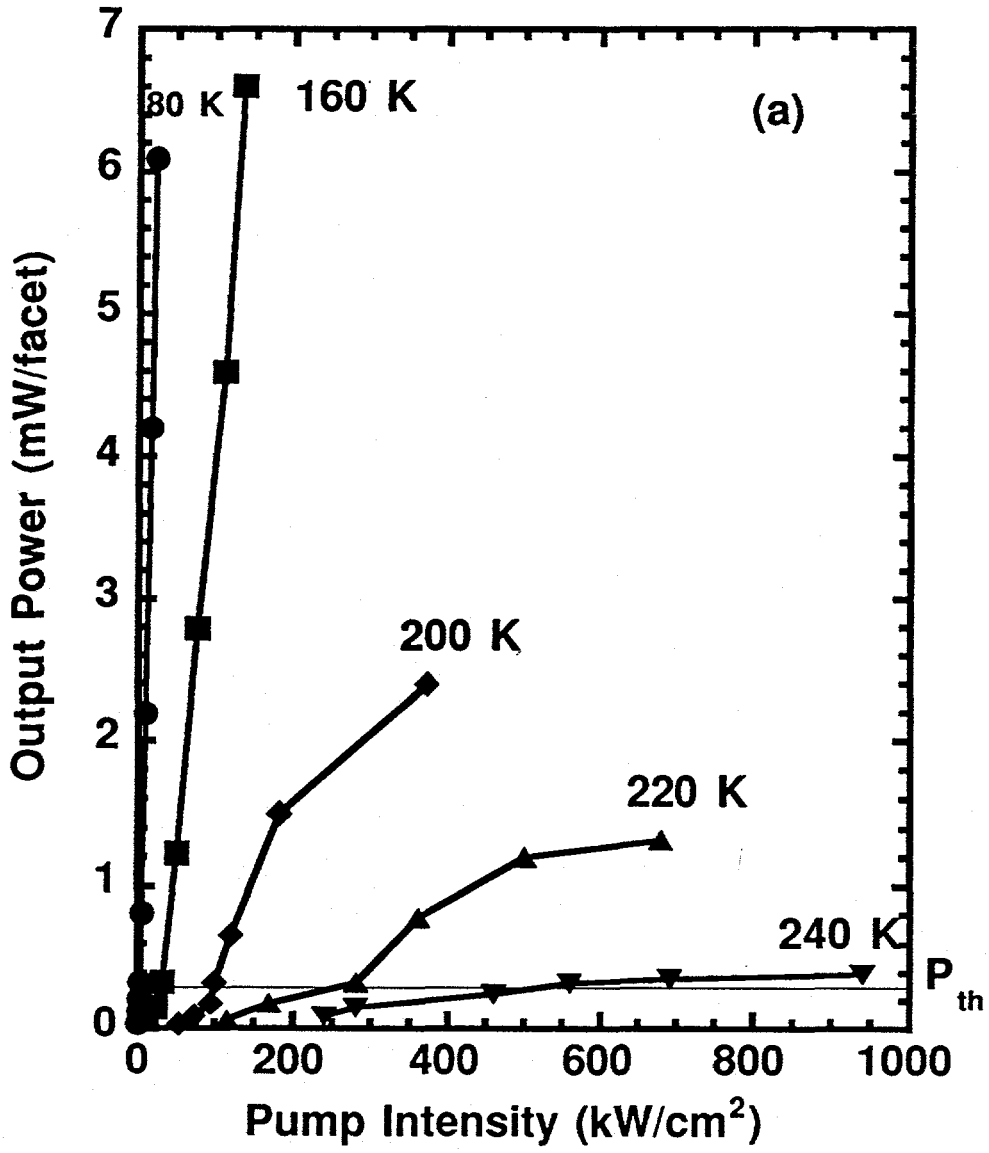
80 K
160 K
(a)
200 K
220 K
240 K
P th
Output Power (mW/facet)
Pump Intensity (kW/cm2)
0
1
2
3
4
5
6
7
0
200
400
600
800
1000

Figure 7 (a)

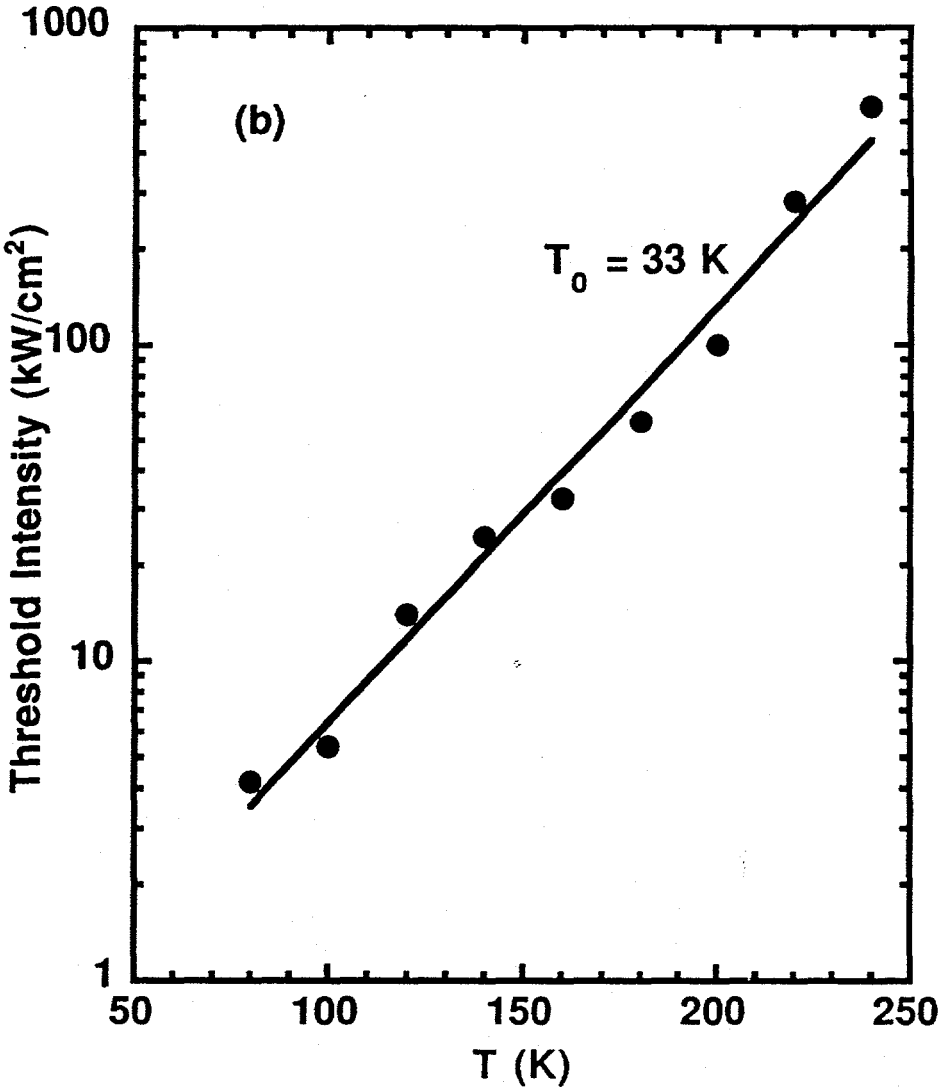
1000
100
10
1
(b)
T_0 = 33 K
Threshold Intensity (kW/cm^2)
50
100
150
200
250
T (K)

Figure 7 (b)